Review

Nuclear Medicine Review 2011, 14, 2: 90–95
10.5603/NMR.2011.00022

ISSN 1506–9680

VIA MEDICA

Contribution of [64Cu]-ATSM PET in molecular imaging of tumour hypoxia compared to classical [18F]-MISO — a selected review

Mickaël Bourgeois[1, 2], Holisoa Rajerison[1], François Guerard[1], Marie Mougin-Degraef[1], Jacques Barbet[1, 2], Nathalie Michel[2], Michel Cherel[1], Alain Faivre-Chauvet[1], Jean-François Gestin[1]

[1]Centre de Recherche en Cancérologie Nantes-Angers, Inserm, Université de Nantes, Nantes, France
[2]GIP ARRONAX, Saint-Herblain, France

[Received 13 VII 2011; Accepted 16 XI 2011]

Abstract

During the carcinogenesis process, tumour cells often have a more rapid proliferation potential than cells that participate in blood capillary formation by neoangiogenesis. As a consequence of the poorly organized vasculature of various solid tumours, a limited oxygen delivery is observed. This hypoxic mechanism frequently occurs in solid cancers and can lead to therapeutic resistance. The present selected literature review is focused on the comparison of two positron emitting radiopharmaceuticals agents, which are currently leaders in tumour hypoxia imaging by PET. [^{18}F]-fluoromisonidazole (= FMISO) is most commonly used as an investigational PET agent with an investigational new drug exemption from the FDA, while [^{64}Cu]-diacetyl-bis(*N*^{4}-methylthiosemicarbazone) (^{64}Cu-ATSM) has been presented as an alternative radiopharmaceutical not yet readily available. The comparison of these two radiopharmaceutical agents is particularly focused on isotope properties, radiopharmaceutical labelling process, pharmacological mechanisms, dosimetry data in patients, and clinical results in terms of image contrast. PET imaging has demonstrated a good efficacy in tumour hypoxia imaging with both FMISO and Cu-ATSM, but FMISO has presented too slow an in vivo accumulation and a weak image contrast of the hypoxia area. Despite a less favourable dosimetry, ^{64}Cu-ATSM appears superior in terms of imaging performance, calling for industrial and clinical development of this innovative radiopharmaceutical.

Key words: cancer, [Copper-64]-ATSM, [Fluorine-18]-MISO, hypoxia, positron emission tomography, tumour microenvironment, radiopharmaceutical

Nuclear Med Rev 2011; 14, 2: 90–95

Correspondence to: Mickaël Bourgeois PharmD, PhD
Centre de Recherche en Cancérologie Nantes-Angers, IRT-UN
8 quai Moncousu, 44007 Nantes cedex 1, France
Tel: +33 2 28 08 02 18, fax: +33 2 28 08 02 04
e-mail: bourgeois@arronax-nantes.fr

Introduction

During the carcinogenesis process of a wide range of solid tumours, tumour cells often have a more rapid proliferation potential than the cells that form blood capillaries by neoangiogenesis. As a consequence of this poorly organized vasculature, a hypoxia area is often observed due to the limited delivery of oxygen (Figure 1) in a population of cells distant from blood vessels (> 100 mm from the closest blood vessel [1]).

Hypoxia in the tumour microenvironment is an extensively studied parameter because this lack of oxygen has negative implications for clinical outcome. The effects of hypoxia are related to two major events: 1 — hypoxia raises genetic instability and more aggressive phenotypes with bad prognosis for patients, and 2 — hypoxic cells are more resistant to radiotherapy and chemotherapy treatments (consequence of poor vascularization [2]). The increased resistance to radiotherapy (Figure 2) has been particularly studied in head and neck cancers and cervical carcino-

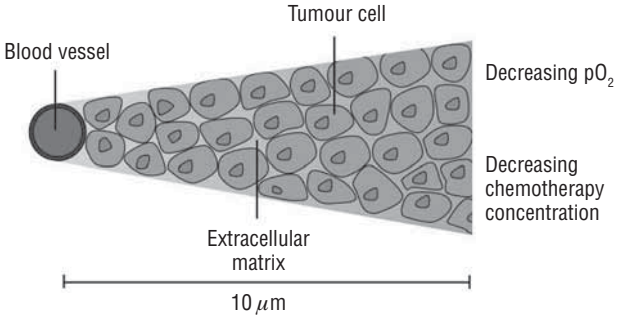

Figure 1. Hypoxia consequences in tumour cells distant from blood vessels.

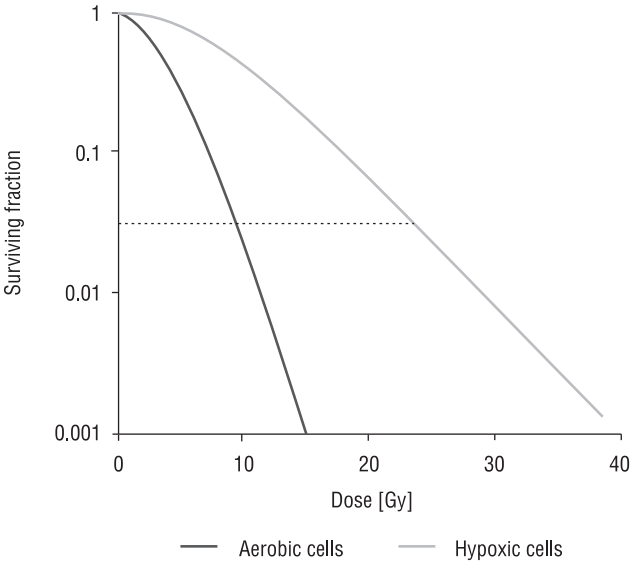

Figure 2. Cell survival-curve for aerobic and hypoxic cells.

mas [3, 4] and is associated with the loss of oxygen enhancement effect during radiotherapy.

The radiobiological mechanism by which ionizing radiations kill cells is mostly based on DNA damage, particularly DNA double strand breaks. This damage results from ionization either in or very close to the DNA molecule, producing a radical on the DNA (DNA$^{\ddot{y}}$). This radical is then engaged either in an oxidation process into aerobic cells resulting in permanent damage, or in a reduction process into hypoxic cells [5] mostly by thiol-containing compounds that can restore DNA and lead to tumour cell survival.

Over the years, several different methods have been developed to assess the *in vivo* hypoxic level of tumours. The polarographic oxygen electrode (most commonly known as the "Eppendorf electrode") was used as the gold standard and has been extensively employed for quantifying hypoxia at different positions in tumours and within a short time frame in both animal studies and human tumours [6, 7]. However, this method presents some major drawbacks. It is an invasive technique limited to accessible tumours with sufficient size with a risk of tissue disruption and is known to present large inter-observer variability [8]. Another invasive method based on biopsy immunohistochemical analysis of hypoxia-inducing factors-1α (HIF-1α) is used to investigate the hypoxia status of tumours. HIF-1α is the major transcription factor of genes that are involved in angiogenesis, glucose metabolism, cell proliferation/survival, and invasion/metastasis and was found overexpressed in human cancers as a result of intratumoural hypoxia [9].

In recent decades, investigations into alternative, non-invasive imaging methods for measuring pO_2 have been studied [10]. The use of positron emission tomography (PET) has led to a number of promising positron emitter radiopharmaceuticals [11–13]. The purpose of the present selected literature review is focused on the comparison of the two positron emitter radiopharmaceutical agents which are currently the leaders in PET imaging of tumour hypoxia: [^{18}F]-fluoromisonidazole (= [^{18}F]-FMISO) used as a reference and the innovative [^{64}Cu]-diacetyl-bis(*N*^{4}-methylthiosemicarbazone) (= [^{64}Cu]-ATSM). Among the different tumour hypoxia PET radiotracers, we choose these two compounds for the following reasons: [^{18}F]-FMISO is the most used radiopharmaceutical in this clinical indication, it is also the classical reference for nitroimidazole compounds, while ATSM seems to be an innovative compound for hypoxia imaging which could be labelled with some copper positron emitter radioactive isotopes like $^{60/61/62/64}$Cu. The metabolism and pharmacological pathway of ATSM-Cu complex is the same for all the copper isotopes, and the choice for clinical use between these isotopes is based on physical properties. The physical and production properties of $^{60/61/62/64}$Cu isotopes are summarized in Table 1.

Briefly, copper-60, 61, and 62 present too short a half-life for essential wide delivery of routine clinical isotopes in nuclear medicine practice. However, copper-62 presents an alternative production means by the ^{62}Zn/^{62}Cu generator. The advantage of this generator is the half-life of ^{62}Zn (9.2 hours), but the major drawback is the small cross section of the ^{62}Zn cyclotron production leading to an important production cost which will limit its clinical use. Fur-

Table 1. Physical and production properties of positron emitter copper isotopes [14–16]

Copper Isotopes	Half-life	Branching ratio of b^+	Max energy of b^+ [keV]	Max intrinsic resolution in tissue [mm]	Nuclear production reaction	Energy for max cross section [MeV\	Production cross section [mbarn]
^{60}Cu	23.7 min	93%	1980.8	9.9	^{60}Ni(p,n)^{60}Cu	12.5	308
^{61}Cu	3.3 h	62%	1215.2	5.1	^{61}Ni(p,n)^{61}Cu	11.0	407
^{62}Cu	9.7 min	98%	2926.0	16.6	^{62}Ni(p,n)^{62}Cu	10.7	1390
					^{63}Cu(p,2n) ^{62}Zn ®^{62}Cu	24.5	63
^{64}Cu	12.7 h	18%	653.0	2.2	^{64}Ni(p,n)^{64}Cu	10.6	837

Table 2. Physical properties of fluorine-18 and copper-64

Isotopes	Half-life	Branching ratio of b^+	Mean energy of b^+ [keV]	Max. energy of b^+ [keV]	Other emission (branching ratio)
^{18}F	109.77 min	100%	249.8	633.05	/
^{64}Cu	12.701 h	17.6%	278.21	653.03	Auger electron (41%) γ (0.5%) β (38.5%)

thermore, copper-60, 61, and 62 present an important b^+ energy and consequently a poor intrinsic resolution. Despite the fact that copper-64 presents a low positron branching ratio (17.6%) and relatively poor dosimetric characteristics, for clinical possibilities, in this review we focused on ^{64}Cu because this isotope presents the best compromise between adapted physical properties (sufficiently long half-life, better intrinsic image resolution with low b^+ maximal energy) and good production yield (reasonable production costs). The main objective of this study is to demonstrate the potential clinical role of [^{64}Cu]-ATSM compared to [^{18}F]-FMISO in the imaging of tumour hypoxia. To compare [^{18}F]-FMISO and [^{64}Cu]-ATSM radiopharmaceuticals agents, we focused in particular on isotope properties, radiopharmaceutical labelling processes, cell hypoxia accumulation pathways, dosimetric data on patients, and clinical results in terms of image contrast.

Comparisons of [^{18}F]-FMISO and [^{64}Cu]-ATSM

Isotope properties and production parameters

Both isotopes, fluorine-18 and copper-64, are produced by cyclotron irradiation. Fluorine-18 is usually obtained by the $^{18}O(p,n)^{18}F$ reaction. A maximum cross section of about 600 mbarn is obtained with a proton beam of about 5 MeV [17]. Copper-64 is mainly obtained by the $^{64}Ni(p,n)^{64}Cu$ nuclear reaction. This cyclotron reaction requires a proton beam of about 11 MeV and presents a good production yield with a cross section of about 700 mbarn [15, 16]. With the ARRONAX cyclotron (a high energy and high intensity multi-particle accelerator located in Nantes, France) another reaction route, ^{64}Ni (d,2n), is used. The excitation function looks attractive, with a maximum cross section of 800 mbarn at 16 MeV [18]. Targets are made of enriched ^{64}Ni (more than 96%) electroplated onto gold backing. Since ^{64}Ni is expensive, it is necessary to recycle it in order to reduce costs. Moreover, a comparison of cross section data between the two reaction routes points out a good yield for the $^{64}Ni(d,2n)$ reaction with a thinner deposit of ^{64}Ni, which reduces cost too [19]. The physical characteristics of these two isotopes are given in Table 2.

Radiopharmaceutical labelling

To date, the most commonly used route for radiolabelling of 3-[^{18}F]fluoro-1-(2'-nitro-1'-imidazolyl)-2-propanol (=[^{18}F]-fluoromisonidazole) is the nucleophilic substitution of the tosylate-leaving group by no-carrier added [^{18}F]-fluoride of the tetrahydropyranyl-protected precursor 1-(2'-nitro-1'-imidazolyl)-2-O-tetrahydropyranyl-3-O-toluenesulphonylpropanediol (NITTP), followed by the hydrolysis of the protecting group with 1M HCl [20]. The synthesis procedure is summarized in Figure 3A.

The classical way to prepare [^{64}Cu]-diacetyl-bis(N^4-methyl-thiosemicarbazone) (= [^{64}Cu]-ATSM) is the addition of 1.5 ml of 1 M sodium acetate on the dry residue of purified copper chloride ($CuCl_2$) followed by the addition of H_2-ATSM in DMSO [21]. The synthesis procedure is summarized in Figure 3B.

In terms of international pharmaceutical regulations, both chemical precursors (NITTP and H_2-ATSM are considered as raw materials) for radiolabelling can be purchased from companies that manufacture these products according to good manufacturing practice requirements for active pharmaceutical ingredients for use in clinical trials (International Conference on Harmonisation Q7 chapter 19).

Currently the two radiopharmaceuticals can be prepared by a fully automated procedure in sufficient amounts for clinical practice, with a radiochemical purity greater than 95%, giving a final product that fulfils the criteria of radiopharmaceutical quality (in terms of radionuclidic purity, sterility, and bacterial endotoxin analysis) [20, 21].

Pharmacological mechanism of radiotracer uptake

Both radiopharmaceuticals are lipophilic compounds which, therefore, diffuse rapidly through cell membranes. The two mechanisms of intracellular accumulation are presented in Figure 4.

Briefly, after entering a viable cell, nitroimidazole compounds, like [^{18}F]-FMISO, are reduced to RNO_2 radicals, regardless of the intracellular oxygen level. In the presence of oxygen, the radical is immediately reoxidized, and [^{18}F]-FMISO leaves the cell. However, if the intracellular oxygen concentration is low, the RNO_2 radicals are further reduced to RNHOH compounds that bind covalently to intracellular macromolecules and remain within the cell [22, 23].

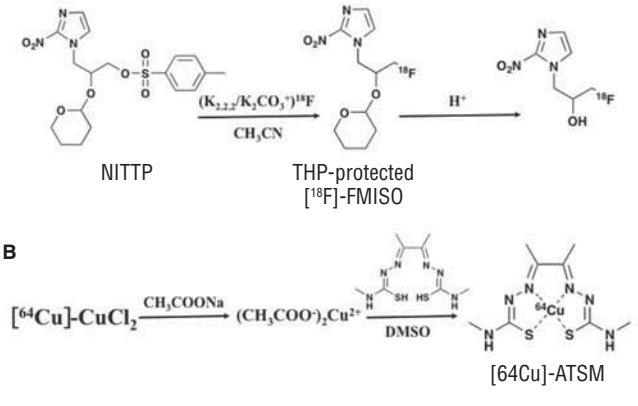

Figure 3A. Radiolabelling of ^{18}F-MISO; **B.** Radiolabelling of ^{64}Cu-ATSM.

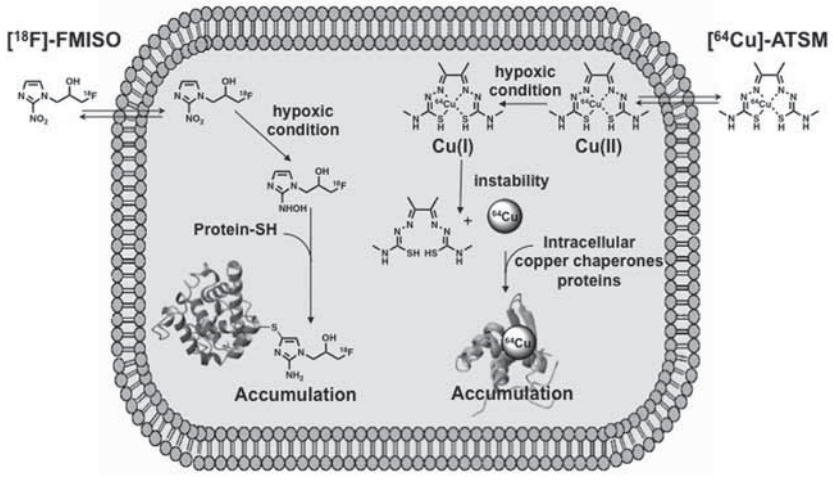

Figure 4. Penetration and intracellular metabolic ways of ^{18}F-MISO (left) and ^{64}Cu-ATSM (right).

The retention mechanism of [^{64}Cu]-ATSM in hypoxic cells has been explored by several groups in the world. The latest development in the elucidation of the pharmacological mechanism is the following. The reduction of [Cu(II)-ATSM] complex by intracellular thiols takes place in both normoxic and hypoxic cells resulting in an unstable [Cu(I)-ATSM]$^-$ complex. The lowest lipophilicity of this negatively charged complex increases its residence time within the cell [24]. In the presence of oxygen (normoxic cells), this unstable species is re-oxidised to a stable [Cu(II)-ATSM] complex and diffuses out of cells. Under hypoxic conditions, the [Cu(I)-ATSM]$^-$ complex slowly dissociates and copper is irreversibly trapped by intracellular copper chaperones proteins (Figure 4) [25–27]. *In vitro* studies have demonstrated that the accumulation time in normoxic cells was two to nine times lower than that in hypoxic cells, depending upon cell line [28]. This explains why, in clinical practice, despite the fact that the ATSM-copper complex is taken up in normoxic cells, a good image contrast is obtained.

Patient dosimetric data

The classical injected activity for a PET image of tumour hypoxia is about 3.7 MBq/kg (maximum 370 MBq) for [^{18}F]-FMISO [29] and 925 MBq for [^{64}Cu]-ATSM [30].

The comparative dosimetric data for internal organs obtained for the two radiotracers in men are given in Table 3 [31, 32] and show a twofold higher total body irradiation and 21-fold higher liver irradiation for [^{64}Cu]-ATSM than [^{18}F]-FMISO. These relatively high dosimetric values for a diagnostic protocol are in the same order of magnitude as the total body dosimetry observed with thallium-201 in stress and rest cardiac imaging [33] and the liver irradiation observed for an abdomen multidetector CT scan procedure (11.5 mSv for a tissue weighting factor of 0.04) [34].

Clinical imaging of hypoxia

The first report on the use of [^{18}F]-FMISO in humans was published in 1992 for three patients with malignant glioma [35]. In 1996, a study assessed the level of hypoxia in a variety of human cancers (37 patients with non-small cell lung cancer, head and neck tumours, prostate tumours, cervical carcinoma, rectal carcinoma, metastatic breast carcinoma, thyroid carcinoma, or metastatic renal cell carcinoma) and concluded that human tumour hypoxia was widely prevalent and highly variable between tumours with the same histology and also between regions within the same tumour [36]. Tissue hypoxia has been determined by PET imaging and quantified in terms of contrast based on tissue-to-blood ratio (T/B) higher than 1.2, 2 hours after radiopharmaceutical administration [37]. Different studies compared [^{18}F]-FMISO uptake with pO_2 measurement from an "Eppendorf electrode" and confirmed, with a good correlation, the use of [^{18}F]-FMISO PET to measure hypoxia in renal cell carcinoma and head and neck cancer but not on human soft tissue tumours [38]. Several clinical studies have used [^{18}F]-FMISO as a prognostic indicator for the survival of a number of patients. The kinetic behaviour of [^{18}F]-FMISO in tumour tissue allowed a good prediction of patient outcome after radiotherapy and prediction of freedom from disease as well as overall survival [39].

Table 3. Comparative patient dosimetric data for [^{18}F]-FMISO [31] and [^{64}Cu]-ATSM [32]

Target organ	[^{18}F]-FMISO [mGy/MBq]	[^{64}Cu]-ATSM [mGy/MBq]
Liver	0.0183	0.390
Kidneys	0.0157	0.088
Spleen	0.0163	0.047
Gallbladder	0.0148	0.068
Adrenals	0.0166	0.032
Heart wall	0.0185	0.029
Pancreas	0.0179	0.056
Upper large intestine	0.0140	0.022
Lungs	0.0099	0.021
Stomach	0.0126	0.021
Total body	0.0126	0.026
Equivalent dose [mSv/MBq]	0.0140	0.036

The utilization of [^{64}Cu]-ATSM is more recent. The first use in a human clinical trial was published in 2000 for patients with lung cancer, and an intense uptake was observed in all cancer patients [40]. For [^{64}Cu]-ATSM, a good image contrast was obtained to a tissue-to-muscle ratio (T/M) threshold of 3.5. This threshold value differentiated patients whose cancer did not recur from those who developed a recurrence after complete therapy [41]. A PET study conducted in patients suffering from cervical cancer comparing [^{64}Cu]-ATSM uptake with tissue molecular markers of hypoxia (vascular endothelial growth factor, cyclo-oxygenase-2, epidermal growth factor, carbonic anhydrase IX) confirmed a good correlation between quantitative PET image and overexpression of the hypoxia molecular factors [42]. In 2001, a study successfully used the ability of [^{64}Cu]-ATSM to delineate hypoxic regions of tumours prior to performing optimal intensity-modulated radiation therapy (IMRT) by delivering a higher dose of radiation to hypoxic regions of the tumour while protecting the healthy margin in the head and the neck of cancer patients [43]. [^{64}Cu]-ATSM has been used in some clinical PET studies and has shown high contrasts levels between hypoxic and normoxic tissues 10–15 minutes post injection, and provided clinically relevant information in terms of chemo/radio-resistance in different tumour sites, such as lung, rectal, or cervical carcinomas (images obtained with ^{60}Cu-ATSM and confirmed with ^{64}Cu-ATSM [44, 45]). Some authors observed variations in image uniformity that could be related to the uptake site (cytosol or mitochondria) or to cell-to-cell biochemistry variations (glycolysis or oxidative reduction pathway). The origin of this cellular accumulation variability is actually unknown but may provide, in the future, information about the phenotype of the cancer cell and finally on the patient outcome [24, 41].

Discussion/Conclusions

The two radiotracers of tumour hypoxia may be obtained with an easy and safe radiolabelling procedure in sufficient a amount for clinical practice. In terms of isotope physical properties, fluorine-18 and copper-64 present the same maximal positron energy, which results in similar close intrinsic image resolution. However, copper-64 presents a longer half-life, which permits easier logistics for PET centres distant from the production cyclotron. Copper-64 production is accessible to a large number of medical cyclotrons that have the possibility to irradiate solid targets. The major drawback of copper-64 is the associated emission of b^- (38.5%), which associates [^{64}Cu]-ATSM with a less favourable dosimetry in comparison to [^{18}F]-FMISO.

Studies using [^{18}F]-FMISO have demonstrated a certain variability, with significant levels of hypoxia in several cancer types but failed to gain wider acceptance for routine clinical application because of a number of limitations, such as:

— slow accumulation in hypoxic tumours;
— low tumour-to-background ratios due to non-specific binding resulting from its relatively high lipophilicity;
— significant non-oxygen dependent metabolism leading to a considerable amount of radioactive metabolites;
— intra-tumoural large uptake variability.

In conclusion, [^{64}Cu]-ATSM has several advantages over other radiopharmaceuticals used for PET of hypoxia, including a simple and rapid method for radiolabelling, faster clearance from normoxic tissues (allowing a short time between injection and imaging), a simple method for quantification, and very good image quality. In various clinical trials, [^{64}Cu]-ATSM provided images of tumour hypoxia that improved the clinical outcome of patients submitted to external beam radiotherapy. The sum of these advantages seems to overcome the less favourable dosimetry of this radiopharmaceutical, and — in conclusion — [^{64}Cu]-ATSM seems to be a good radiopharmaceutical candidate that can be used to obtain high quality images of tumour hypoxia.

Conflict of interests

The authors declared that they have no conflict of interest.

Acknowledgements

This work was supported by grants from Cancéropôle Grand Ouest, the french Agence Nationale de la Recherche (grant ANR-PCV VECRIT, A.F-C) and the french Région des Pays de la Loire (NUCSAN).

References

1. Minchinton AI, Tannock IF. Drug penetration in solid tumours. Nat Rev Cancer 2006; 6: 583–592.
2. Rademakers SE, Span PN, Kaanders JHAM, Sweep FCGJ, van der Kogel AJ, Bussink J. Molecular aspects of tumour hypoxia. Mol Oncol 2008; 2: 41–53.
3. Höckel M, Schlenger K, Mitze M, Schäffer U, Vaupel P. Hypoxia and radiation response in human tumors. Semin Radiat Oncol 1996; 6: 3–9.
4. Nordsmark M, Bentzen SM, Rudat V et al. Prognostic value of tumor oxygenation in 397 head and neck tumors after primary radiation therapy. An international multi-center study. Radiother Oncol 2005; 77: 18–24.
5. Brown JM, Wilson WR. Exploiting tumour hypoxia in cancer treatment. Nat Rev Cancer 2004; 4: 437–447.
6. Brizel DM, Sibley GS, Prosnitz LR, Scher RL, Dewhirst MW. Tumor hypoxia adversely affects the prognosis of carcinoma of the head and neck. Int J Radiat Oncol Biol Phys 1997; 38: 285–289.
7. Gatenby RA, Kessler HB, Rosenblum JS et al. Oxygen distribution in squamous cell carcinoma metastases and its relationship to outcome of radiation therapy. Int J Radiat Oncol Biol Phys 1988; 14: 831–8.
8. Nozue M, Lee I, Yuan F et al. Interlaboratory variation in oxygen tension measurement by Eppendorf "Histograph" and comparison with hypoxic marker. J Surg Oncol 1997; 66: 30–38.
9. Semenza GL. Targeting HIF-1 for cancer therapy. Nat Rev Cancer 2003; 3: 721–732.
10. Padhani AR, Krohn KA, Lewis JS, Alber M. Imaging oxygenation of human tumours. Eur Radiol 2007 avr; 17: 861–872.
11. Mees G, Dierckx R, Vangestel C, Van de Wiele C. Molecular imaging of hypoxia with radiolabelled agents. Eur J Nucl Med Mol Imaging 2009; 36: 1674–1686.
12. Padhani A. PET imaging of tumour hypoxia. Cancer Imaging 2006; 6: S117–S121.
13. Lewis JS, Welch MJ. PET imaging of hypoxia. Q J Nucl Med 2001; 45: 183–188.
14. Uddin MS, Khandaker MU, Kim KS, Lee YS, Kim GN. Excitation functions of the proton induced nuclear reactions on natZn up to 40 MeV. Nucl Instrum Methods Phys Res B 2007; 258: 313–320.
15. Szelecsényi F, Blessing G, Qaim SM. Excitation functions of proton induced nuclear reactions on enriched 61Ni and 64Ni: Possibility of

production of no-carrier-added 61Cu and 64Cu at a small cyclotron. Appl Radiat Isot 1993; 44: 575–580.
16. Adam Rebeles R, Van den Winkel P, Hermanne A, Tárkányi F. New measurement and evaluation of the excitation function of 64Ni(p,n) reaction for the production of 64Cu. Nucl Instrum Methods Phys Res B 2009; 267: 457–461.
17. Hess E, Takács S, Scholten B, Tárkányi F, Coenen HH, Qaim SM. Excitation function of the18O(p,n)18F nuclear reaction from threshold up to 30 MeV. Radiochim Acta 2001; 89: 357.
18. Zweit J, Smith AM, Downey S, Sharma HL. Excitation functions for deuteron induced reactions in natural nickel: production of no-carrier-added 64Cu from enriched 64Ni targets for positron emission tomography. Int J Rad Appl Instrum A 1991; 42: 193–197.
19. Michel N, Alliot C, Audouin N et al. Production of 64Cu via 64Ni(d,2n)64Cu for medical applications. Proceeding of the 7ICI conference (Moscow–Russia) 2011.
20. Nandy S, Rajan MGR, Korde A, Krishnamurthy NV. The possibility of a fully automated procedure for radiosynthesis of fluorine-18-labeled fluoromisonidazole using a simplified single, neutral alumina column purification procedure. Appl Radiat Isot 2010; 68: 1937–1943.
21. Matarrese M, Bedeschi P, Scardaoni R et al. Automated production of copper radioisotopes and preparation of high specific activity [(64)Cu]Cu-ATSM for PET studies. Appl Radiat Isot 2010; 68: 5–13.
22. Smith BR, Born JL. Metabolism and excretion of [3H]misonidazole by hypoxic rat liver. Int J Radiat Oncol Biol Phys 1984; 10: 1365–1370.
23. Franko AJ, Garrecht BM. Misonidazole retention by normal tissues: a distinction between label on the ring and side chain. Int J Radiat Oncol Biol Phys 1986; 12: 1259–1262.
24. Dearling JLJ, Packard AB. Some thoughts on the mechanism of cellular trapping of Cu(II)-ATSM. Nucl Med Biol 2010; 37: 237–243.
25. Dearling JLJ, Lewis JS, Mullen GED, Welch MJ, Blower PJ. Copper bis(thiosemicarbazone) complexes as hypoxia imaging agents: structure-activity relationships. J Biol Inorg Chem 2002; 7: 249–259.
26. Dence CS, Ponde DE, Welch MJ, Lewis JS. Autoradiographic and small-animal PET comparisons between (18)F-FMISO, (18)F-FDG, (18)F-FLT and the hypoxic selective (64)Cu-ATSM in a rodent model of cancer. Nucl Med Biol 2008; 35: 713–720.
27. Maurer RI, Blower PJ, Dilworth JR, Reynolds CA, Zheng Y, Mullen GED. Studies on the Mechanism of Hypoxic Selectivity in Copper Bis(Thiosemicarbazone) Radiopharmaceuticals. J Med Chem 2002; 45: 1420–1431.
28. Burgman P, O'Donoghue JA, Lewis JS, Welch MJ, Humm JL, Ling CC. Cell line-dependent differences in uptake and retention of the hypoxia-selective nuclear imaging agent Cu-ATSM. Nucl Med Biol 2005; 32: 623–630.
29. Rajendran JG, Schwartz DL, O'Sullivan J et al. Tumor hypoxia imaging with [F-18] fluoromisonidazole positron emission tomography in head and neck cancer. Clin Cancer Res 2006; 12: 5435–5441.
30. Lewis JS, Laforest R, Dehdashti F, Grigsby PW, Welch MJ, Siegel BA. An imaging comparison of 64Cu-ATSM and 60Cu-ATSM in cancer of the uterine cervix. J Nucl Med 2008; 49: 1177–1182.
31. Graham MM, Peterson LM, Link JM et al. Fluorine-18-Fluoromisonidazole radiation dosimetry in imaging studies. J Nucl Med 1997; 38: 1631–1636.
32. Laforest R, Dehdashti F, Lewis JS, Schwarz SW. Dosimetry of 60/61/62/64Cu–ATSM: a hypoxia imaging agent for PET. Eur J Nucl Med Mol Imaging 2005; 32: 764–770.
33. Flotats A, Knuuti J, Gutberlet M et al. Hybrid cardiac imaging: SPECT/CT and PET/CT. A joint position statement by the European Association of Nuclear Medicine (EANM), the European Society of Cardiac Radiology (ESCR) and the European Council of Nuclear Cardiology (ECNC). Eur J Nucl Med Mol Imaging 2011; 38: 201–212.
34. ICRP. Chapter 2. Ann ICRP 2007; 37: 27–37.
35. Valk PE, Mathis CA, Prados MD, Gilbert JC, Budinger TF. Hypoxia in human gliomas: demonstration by PET with fluorine-18-fluoromisonidazole. J Nucl Med 1992; 33: 2133–2137.
36. Rasey JS, Koh WJ, Evans ML et al. Quantifying regional hypoxia in human tumors with positron emission tomography of [18F]fluoromisonidazole: a pretherapy study of 37 patients. Int J Radiat Oncol Biol Phys 1996; 36: 417–428.
37. Koh WJ, Rasey JS, Evans ML, et al. Imaging of hypoxia in human tumors with [F-18]fluoromisonidazole. Int J Radiat Oncol Biol Phys 1992; 22: 199–212.
38. Bentzen L, Keiding S, Nordsmark M et al. Tumour oxygenation assessed by 18F-fluoromisonidazole PET and polarographic needle electrodes in human soft tissue tumours. Radiother Oncol 2003; 67: 339–344.
39. Cher LM, Murone C, Lawrentschuk N et al. Correlation of hypoxic cell fraction and angiogenesis with glucose metabolic rate in gliomas using 18F-fluoromisonidazole, 18F-FDG PET, and immunohistochemical studies. J Nucl Med 2006; 47: 410–418.
40. Takahashi N, Fujibayashi Y, Yonekura Y et al. Evaluation of ^{62}Cu labeled diacetyl-bis(N4-methylthiosemicarbazone) as a hypoxic tissue tracer in patients with lung cancer. Ann Nucl Med 2000; 14: 323–328.
41. Dehdashti F, Grigsby PW, Mintun MA, Lewis JS, Siegel BA, Welch MJ. Assessing tumor hypoxia in cervical cancer by positron emission tomography with 60Cu-ATSM: relationship to therapeutic response — a preliminary report. Int J Radiat Oncol Biol Phys 2003; 55: 1233–1238.
42. Grigsby PW, Malyapa RS, Higashikubo R et al. Comparison of molecular markers of hypoxia and imaging with (60)Cu-ATSM in cancer of the uterine cervix. Mol Imaging Biol 2007; 9: 278–283.
43. Chao KS, Bosch WR, Mutic S et al. A prospective study on tumor hypoxia kinetics to implement hypoxic imaging-guided IMRT. Int J Radiat Oncol Biol Phys 2001; 51 (3 suppl 1): 83.
44. Dehdashti F, Mintun MA, Lewis JS et al. In vivo assessment of tumor hypoxia in lung cancer with 60Cu-ATSM. Eur J Nucl Med Mol Imaging 2003; 30: 844–850.
45. Dietz DW, Dehdashti F, Grigsby PW et al. Tumor hypoxia detected by positron emission tomography with 60Cu-ATSM as a predictor of response and survival in patients undergoing Neoadjuvant chemoradiotherapy for rectal carcinoma: a pilot study. Dis Colon Rectum 2008; 51: 1641–1648.